An in vitro study of magnetization transfer and relaxation rates of hematoma.

J M Gomori, R I Grossman, T Asakura, M D Schnall, S Atlas, G Holland and R L Mittl, Jr

AJNR Am J Neuroradiol 1993, 14 (4) 871-880
http://www.ajnr.org/content/14/4/871

An in Vitro Study of Magnetization Transfer and Relaxation Rates of Hematoma

John M. Gomori,[1,3] Robert I. Grossman,[1] Toshio Asakura,[2] Mitchell D. Schnall,[1] Scott Atlas,[1] George Holland,[1] and Robert L. Mittl, Jr.[1]

PURPOSE: To assess, in an in vitro model of acute hematoma, whether hemoglobin immobilization by clot and red cell membrane aging can account for the T2 shortening usually attributed to deoxyhemoglobin. **METHODS:** Clotted and heparinized blood samples were packed (100% hematocrit). The apparent magnetization transfer rate (AMTR), T1 and T2 relaxation rates of the samples, and images with a volunteer's head were obtained at 1.5 T. **RESULTS:** The AMTR and T1 and T2 relaxation rates were unaffected by the presence of clot. The AMTR was unaffected by red cell aging. The diamagnetic packed blood samples, which are much denser than brain, were isointense to gray matter on T2-weighted images and had about one-fifth the AMTR of white matter. **CONCLUSIONS:** Hemoglobin immobilization by clot structure or red cell contraction with aging is insignificant and does not contribute to the T2 shortening of acute hematoma. The low AMTR and T2 relaxation rates of diamagnetic blood appear to be caused by the mobility of hemoglobin and by the red cell's lack of immobile macromolecular structures such as those associated with nucleated brain cells.

Index terms: Hematoma; Blood, coagulation; Blood, magnetic resonance; Magnetic resonance, tissue characterization; Magnetic resonance, experimental

AJNR 14:871–880, Jul/Aug 1993

The magnetic resonance (MR) of acute and subacute hematomas is dominated by the paramagnetic effects of deoxyhemoglobin and methemoglobin. Acute hematomas are characterized by the susceptibility heterogeneity of intracellular deoxyhemoglobin (1, 2). Relative to brain parenchyma, it increases their T2 relaxation rate on high field spin-echo images (1, 2) and their T2* relaxation rate on gradient-echo images (3, 4, 5) at most field strengths. However, on low field spin-echo MR, on which the effects of susceptibility heterogeneity are negligible, the brain's T2 relaxation rate is greater than or equal to that of compact acute hematomas, despite the brain's lower computed tomography (CT) density (1, 6). This elevation of the T2 relaxation rates and T1/T2 ratios of the brain and other tissues compared with protein solution of equivalent density appears to be caused by the immobility of their cellular macromolecular structures, which accelerates the T2 relaxation rate of the surrounding free water protons (7–21). Although immobilization also shortens the macromolecular proton T2 (22) to the point of invisibility on conventional MR, it does increase its magnetization transfer rate (14, 16, 19, 22). Fortunately, magnetization transfer, a phenomenon unique to the immobile protons, can be detected as a decrease in the free water signal upon saturation of the immobile protons.

Interest in magnetization transfer has been excited by the studies of Balaban et al (15, 16, 20, 21). Concurrently, a recent report has advocated a reassessment of the importance of susceptibility heterogeneity for the hypointensity of acute hematomas on T2-weighted spin-echo images (23). It was proposed that immobilization of hemoglobin by clot structure, red cell dehydration, and related processes may be the major contributor

Received July 22, 1992; revision requested December 28, received March 29, 1993, and accepted April 6.

[1] Department of Radiology, Hospital of the University of Pennsylvania, 3400 Spruce Street, Philadelphia, PA 19104.

[2] Department of Hematology, Children's Hospital, Philadelphia, PA 19104.

[3] Department of Radiology, Hadassah University Hospital, PO Box 12000, Jerusalem 91120, Israel. Address reprint requests to John M. Gomori, MD.

AJNR 14:871–880, Jul/Aug 1993 0195-6108/93/1404-0861

to T2 relaxation. To date, such processes have not been demonstrated to be significant (24–30). However, if they occur they should increase the magnetization transfer rate, a sensitive indicator of macromolecular immobility.

This study uses the apparent magnetization transfer rates (AMTRs) as well as the more familiar T1 and T2 relaxation rates to assess the significance of the previously mentioned factors in producing the hypointensity of T2-weighted images of acute hematoma. The AMTR is an approximate measure for k_{for} term used in the spectroscopic literature. Packed blood samples were used in this study for four reasons: 1) the immobilization of hemoglobin was proposed to occur in compact hematomas (23); 2) the T2 relaxation rate and AMTR of protein solutions increase with concentration (17, 31); 3) packing blood to a hematocrit of 100% eliminates susceptibility heterogeneity (32); and 4) the final packing of blood by centrifugation is more reproducible than the preceding sedimentation or clot retraction.

Materials and Methods

Sample Preparation

Forty-milliliter aliquots of fresh blood were obtained from volunteers, and samples of different blood states were prepared. The unclotted samples were heparinized. The oxygenated samples were prepared by bubbling with humidified oxygen. However, some of the oxyhemoglobin samples became partially deoxygenated over hours (33), perhaps because of white cell metabolism. Because there is no difference in the relaxation rates of oxyhemoglobin and carbonmonoxyhemoglobin blood (34), we used the more stable carbonmonoxyhemoglobin as the diamagnetic hemoglobin state for this study. Carbonmonoxyhemoglobin samples were prepared by bubbling with carbon monoxide. Deoxygenated samples were prepared by bubbling with humidified nitrogen followed by the addition of a few drops of isotonic buffered sodium dithionite. Methemoglobin samples were prepared by the addition of a few drops of isotonic buffered sodium nitrate.

Clot formation was expedited by the addition of a few drops of isotonic buffered $CaCl_2$. Osmolality and pH were modified by resuspending centrifuged carbonmonoxyhemoglobin blood samples twice with buffered solutions of different osmolality or pH. Rouleaux formation, another immobilizing process, was also inhibited by the exchange of plasma with isotonic buffered saline (35–37). However, rouleaux formation should have negligible effects in packed samples. Two samples were prepared of each blood state. They were centrifuged at about 1000 × *g* for 10 minutes, and the supernatant was removed. Then in one of the samples the red cells were lysed by two freeze-thaw cycles.

Plasma clot formation was expedited by a few drops of isotonic buffered $CaCl_2$ and the addition of 1 mg protamine to 40 ml plasma without platelets. A retracted plasma clot was formed similarly in plasma with platelets. The retracted clot was centrifuged and the liquid supernatant removed.

MR

A 1.5-T clinical imager was used (Signa, GE, Madison, WI). The T1 and T2 relaxation rates were measured using 5-mm-thick single section images. The T1 rates were obtained from a series of three images with a repetition time (TR) of 200, 800, and 2000 msec, and with an echo time (TE) of 11 msec. The T2 rates were obtained from images with a TR of 3500 msec and TE of 22.5, 45, 67.5, and 90 msec. Images were also obtained with a TR of 3500 with a single echo at a TE of 90 msec. The other image parameters were acquisition matrix 192 × 256, number of excitations 1, and field of view 30 to 32 cm. The body coil was used for a more uniform radio frequency field through the blood and plasma sample array.

The blood and plasma sample array was also imaged with a volunteer's head (500/12/1 and 3000/20–90/1 (TR/TE/excitations), 128 × 256 matrix, field of view 32 cm) with 10-mm-thick section with 2.5 mm gap using the body coil.

Three-point T1 and four-point T2 calculations were performed in four separate regions of each sample using the imager software. The regions of interest were of 0.5 cm diameter (sample diameter 2.5 cm). Similar measurements were performed on periventricular white matter and basal ganglia gray matter in the volunteer's brain images. The presence of susceptibility heterogeneity in the samples was assessed by the decrease in T2 relaxation rate with cell lysis and with shortening of the interecho interval from 90 to 22.5 msec (2, 28).

Magnetization Transfer

Theory (15, 20, 38, 39, 40). Magnetization transfer links the immobile proton pool to the free water protons and modifies the Bloch equation to: $dM_z/dt = (M_0 - M_z)/T1 + (MTR_b)M_{zb} - (MTR)M_z$, where M_z is the longitudinal magnetization of the free water protons and M_0 is its equilibrium value, M_{zb} is the immobile proton longitudinal magnetization and MTR and MTR_b are the magnetization transfer rates of the free water protons and the immobile protons respectively.

If the immobile protons are selectively saturated ($M_{zb} = 0$) the modified Bloch equation simplifies to: $dM_z/dt = (M_s - M_z)/T1_{sat}$, where $1/T1_{sat} = 1/T1 + MTR$, and M_s is the new equilibrium longitudinal magnetization of the free water protons under continuous and complete saturation of the immobile protons. Then: $MTR = MTC/T1_{sat} = [(MTC)/(1 - MTC)]/T1$, where $MTC = (M_0 - M_s)/M_0$.

Classic frequency selective saturation of the immobile protons is not possible, because both proton pools have the same resonant frequency. Preferrential saturation of the immobile protons is accomplished by radio frequency

irradiation that is sensitive to the marked difference in the T2 relaxation rates of the two proton populations. These pulses are soft; that is, long relative to the T2 of the immobile protons. Two pulse categories are used: on-resonance and off-resonance pulses. On resonance pulses are of intermediate length; that is, soft relative to the immobile protons and hard relative the free water protons. These cause partial saturation of the immobile protons and rotate the free water protons a multiple of 360°, effectively 0°. Off-resonance techniques use long off-resonance pulses that are soft relative to both proton populations. However, off resonance causes greater saturation of the immobile protons. Both techniques may be limited in the achievable saturation of the immobile protons for any given bound on the saturation of the free water protons (bleed-over). Incomplete saturation of the immobile protons because of these inherent limitations, as well as limitations specific to the MR equipment and pulse sequence used, may make use of the above equations problematic. Until a better theoretic understanding (eg 40a) is attained, the accuracy of MTC and MTR measurements using the above equations is uncertain. We chose to call our measurements apparent MTC and MTR to emphasize their relative nature and to condition their comparison with measurements obtained by other pulse sequences.

Technique

To study magnetization transfer we used the off-resonance technique for the preferential saturation of the immobile protons. Images were acquired with a three-dimensional spoiled gradient-echo (GRASS, GE) sequence (110/6, flip angle $\alpha_1 = 10°$, 28 × 192 × 256 matrix with 5-mm section width) with and without a presaturation pulse 2 kHz off water resonance applied without any magnetic field gradients (38). The presaturation pulse consisted of 19 msec single-cycle sync pulse with an average B_1 intensity of 3.7×10^{-6} T. The interval between the end of the saturation pulse and the beginning of each excitation was approximately 1 msec. This saturation pulse, designed to saturate immobile macromolecular protons, which have a very broad MR peak, caused less than 1% loss of signal in saline and less than 5% loss of signal in 0.3 mM $MnCl_2$ with a T1 of 400 msec and T2 of 37 msec.

For comparison with the blood samples, bovine serum albumin (BSA) solutions with protein weight fractions of 0.2, 0.33, and 0.5 were prepared. The blood samples with different osmolalities and pHs, the BSA samples, and a volunteer's head were then studied separately of each other with exactly the same sequences as used for the blood and plasma samples. Then the three-dimensional spoiled gradient echo sequence with the presaturation pulse was repeated using a flip angle of $\alpha_2 = 55°$. M_0 is the intensity without the presaturation pulse, and M_s is the intensity with the presaturation pulse. The AMTC and the AMTR were calculated in three separate regions of interest in each sample as follows:

$$AMTC = (M_0(\alpha_1) - M_s(\alpha_1))/M_0(\alpha_1)$$

$$R = M_s(\alpha_2)/M_s(\alpha_1)$$

$$AT1_{sat} = -\frac{1}{TR} \ln \left\{ \frac{1}{\cos\alpha_2} \left[\frac{\frac{\sin\alpha_2}{\sin\alpha_1} - R}{\frac{\tan\alpha_2}{\tan\alpha_1} - R} \right] \right\},$$

where $\alpha_1 = 10°$ and $\alpha_2 = 55°$, AMTR = [(AMTC)/(1 − AMTC)]/T1 or, AMTR = AMTC/$AT1_{sat}$.

The experiments were performed at room temperature. After the experiment the samples were stored at 4°C. At 2 weeks, 4 weeks, and 8 weeks the samples were reimaged at room temperature.

Results

Table 1 presents the magnetization transfer and relaxation rate data of the blood and plasma samples. The AMTRs of all the packed blood samples were much lower than the AMTRs of brain parenchyma. They averaged about 0.3 sec^{-1} versus about 0.9 sec^{-1} for gray matter and 1.5 sec^{-1} for white matter (see Table 6). On the other hand, the T1 relaxation rate of the diamagnetic carbonmonoxyhemoglobin samples with intact cells were similar to that of gray matter, and their T2 relaxation rates were slightly lower that that of gray matter. Clot formation had no effect on the AMTRs or relaxation rates of packed blood, except for a residual susceptibility heterogeneity-induced T2 relaxation enhancement in the deoxyhemoglobin and methemoglobin clots with intact cells. Apparently clot formation trapped some extracellular fluid that was not removed by centrifugation. In plasma, the formation of an unretracted clot also had no effect on the AMTR or relaxation rates. However, the small fully retracted plasma clot had values approaching that of diamagnetic packed blood. The T1 relaxation rate increased with cell lysis in all samples without significant change in the AMTR or T2 relaxation rate, except for the susceptibility related decrease in 1/T2 with lysis of the deoxyhemoglobin and methemoglobin clots as mentioned above.

Table 2 presents the magnetization transfer and relaxation rate data of the carbonmonoxyhemoglobin samples with intact red cells under different osmolality and pH conditions. Marked increase in osmolality increased the AMTR and T2 relaxation rate dramatically. To a lesser extent similar changes occurred with marked increases in pH. There were no significant changes in the AMTRs or T2 relaxation rates with moderate

TABLE 1: Magnesization transfer and relaxation rate data for the blood and plasma samples

	Hb				MHb				HbCO				Plasma		
	1 UI	2 UL	3 CI	4 CL	5 UI	6 UL	7 CI	8 CL	9 UI	10 UL	11 CI	12 CL	13 U	14 C	15 RC
AMTR (sec^{-1})	0.29 ± 0.02	0.29 ± 0.03	0.21 ± 0.01	0.19 ± 0.03	0.30 ± 0.03	0.32 ± 0.05	0.41 ± 0.11	0.29 ± 0.06	0.27 ± 0.02	0.25 ± 0.02	0.35 ± 0.05	0.23 ± 0.04	0.02 ± 0.02	0.02 ± 0.02	0.16 ± 0.08
1/T2 (sec^{-1})	14.6 ± 0.1	14.4 ± 0.1	16.8 ± 0.3	12.7 ± 0.3	18.1 ± 0.2	18.1 ± 0.2	23.6 ± 0.2	15.7 ± 0.0	14.1 ± 0.0	13.9 ± 0.2	14.0 ± 0.3	13.6 ± 0.4	6.6 ± 0.3	6.9 ± 0.3	10.1 ± 9.2
1/T1 (sec^{-1})	1.06 ± 0.01	1.49 ± 0.02	0.88 ± 0.04	1.03 ± 0.06	4.22 ± 0.45	4.90 ± 0.78	3.79 ± 0.23	4.03 ± 0.20	0.91 ± 0.02	1.21 ± 0.03	1.04 ± 0.12	1.15 ± 0.02	0.19 ± 0.17	0.19 ± 0.13	1.17 ± 0.02
AMTC (%)	21.4 ± 0.9	16.5 ± 1.2	19.4 ± 0.1	15.2 ± 1.5	6.7 ± 0.2	6.1 ± 0.3	9.8 ± 2.4	6.7 ± 1.2	23.2 ± 1.5	17.3 ± 1.3	25.4 ± 2.8	16.6 ± 2.6	11.5 ± 0.1	11.4 ± 0.1	16.9 ± 7.2

Note.—Hb = deoxyhemoglobin; MHb = methemoglobin; HbCO = carbonmonoxyhemoglobin; U = unclotted; C = clotted; RC = retracted plasma clot; I = intact red cells; L = lysed red cells.

decrease in osmolality or pH. The T1 relaxation rate was less sensitive to changes in osmolality and pH.

Figure 1 presents the T1- and T2-weighted images of the volunteer's brain with the blood and plasma sample array. Table 3 presents the intensity ratios of the samples to the gray and white matter in Figure 1. The blood and plasma samples were isointense or hyperintense to gray matter on the T2-weighted image. The exceptions were the clotted deoxyhemoglobin and methemoglobin samples with intact cells, which were hypointense to gray matter because of residual susceptibility heterogeneity. On T1-weighted images the deoxyhemoglobin and carbonmonoxyhemoglobin samples were isointense to white matter when the cells were intact and hyperintense when the cell membranes were lysed. The plasma samples were hypointense, and the methemoglobin samples were hyperintense to white matter on T1-weighted images.

As expected, the methemoglobin samples had higher T1 relaxation rates and to a lesser degree higher T2 relaxation rates than the carbonmonoxyhemoglobin and deoxyhemoglobin samples. Although the AMTCs of the methemoglobin samples were decreased, the AMTRs were unaffected by methemoglobin's paramagnetic proton relaxation enhancement.

Over time, there were no significant changes in the AMTRs or T2 relaxation rates of the carbonmonoxyhemoglobin samples with intact cells. Table 4 follows the T1 relaxation rates of the blood samples over time. It shows that with time the T1 relaxation rate increased for the deoxyhemoglobin and carbonmonoxyhemoglobin samples, especially the clots with lysed red cell membranes. In contrast, the T1 relaxation rates of the methemoglobin samples with intact cells, clotted or unclotted, decreased with time, approaching the T1 relaxation rates of nonmethemoglobin samples.

For comparison with the blood samples, Tables 5 and 6 present the magnetization transfer and relaxation rate data of the BSA solutions and of the gray and white matter of the volunteer's brain.

Discussion

Diamagnetic proteins and macromolecular structures affect the free water proton relaxation via interfacial interactions that are rapidly transmitted to the bulk free water by diffusion ex-

TABLE 2: Magnetization transfer and relaxation rate data for packed carbonmonoxyhemoglobin samples that had their plasma replaced by buffered solutions of different osmolality and pH

	pH 7.4			pH 5.9 308 mOsmol	pH 9.0 308 mOsmol
	252 mOsmol I	303 mOsmol I	570 mOsmol I	I	I
AMTR (sec^{-1})	0.25 ± 0.11	0.22 ± 0.10	1.43 ± 0.64	0.23 ± 0.04	0.37 ± 0.11
1/T2 (sec^{-1})	14.5 ± 0.2	16.4 ± 0.2	47.6 ± 0.3	16.4 ± 0.1	21.3 ± 0.2
1/T1 (sec^{-1})	1.04 ± 0.12	1.01 ± 0.16	2.28 ± 0.38	0.99 ± 0.10	1.12 ± 0.10
$1/AT1_{sat}$ (sec^{-1})	1.28 ± 0.23	1.24 ± 0.21	3.46 ± 0.96	1.26 ± 0.13	1.52 ± 0.17
AMTC (%)	19.3 ± 4.5	17.1 ± 3.4	39.8 ± 7.9	18.3 ± 1.9	23.3 ± 4.0

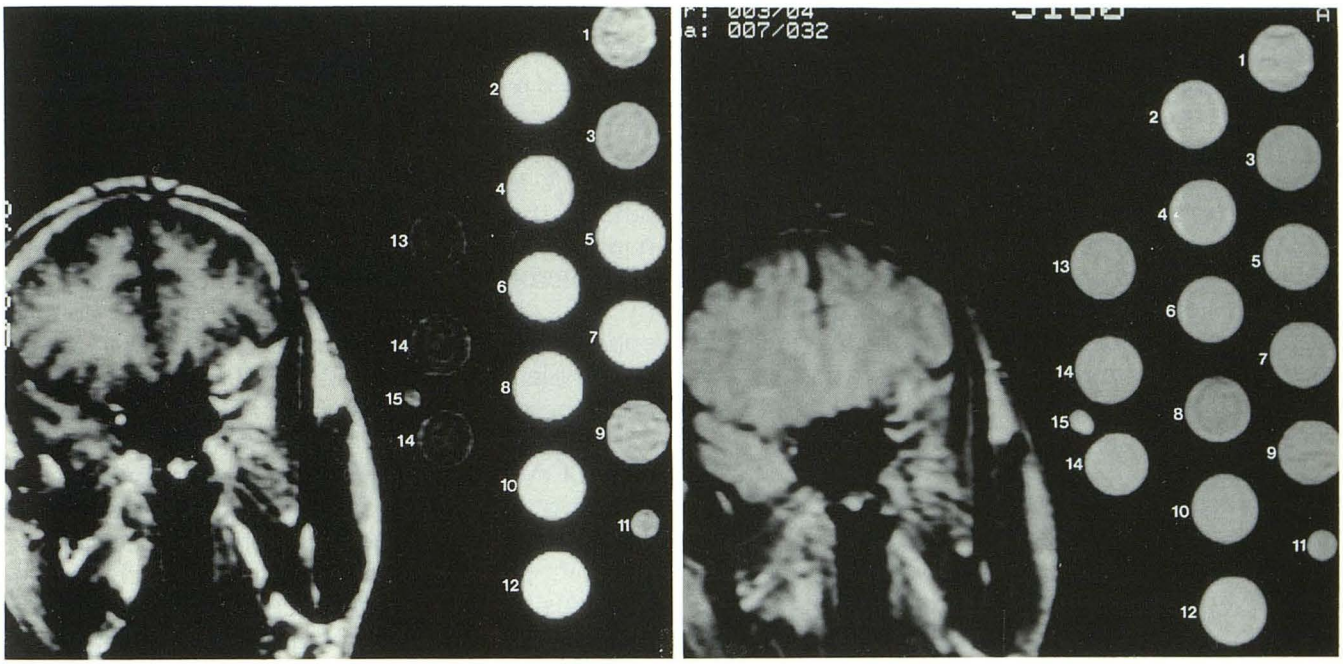

Fig. 1. Coronal MR of the volunteer's head and the blood and plasma sample array. The numbers of the samples correspond to the numbers in Table 1.

A, T1-weighted image, 500/12 (TR/TE). *B* and *C*, Proton density and T2-weighted images, 3000/20–90.

change of water molecules (7–19). Water molecules transiently hydrogen bonded at chemically specific sites on the surface of each protein molecule or macromolecular structure exchange with the free water molecules. In addition, free water protons exchange chemically with labile surface protons (14). The magnetic state of these surface water protons is affected by two major interactions; slowed motion (increased correlation time) and chemical shift. Only a small fraction (1%) (19) of the hydrogen-bonded water is attached long enough (1 μs) to "sense" the slowed motion of the macromolecular surface to which it is attached. Slowed motion increases both the dipolar-dipolar cross-relaxation by the sister proton in the hydrogen-bonded water molecule as well as the dipolar-dipolar cross-relaxation of the water proton by the adjacent protons of the protein molecule or macromolecular structure. The relative importance of the inter-proton cross-relaxation within the hydrogen-bonded water molecule versus that by the adjacent macromolecular proton depends on the respective proton-proton distances and on the respective correlation times; ie, rotational versus translational freedoms of motion.

The T1 and T2 relaxation rates of the free water protons are increased by both cross-relaxation interactions. In addition, cross-relaxation by the adjacent macromolecular protons also transfers longitudinal magnetization between the macromolecular protons and water protons. The consequence of magnetization transfer for the observed T1 relaxation of free water depends on the magnetization transfer rate and on the relative efficiency of the T1 relaxation of the immobile proton pool compared to that of the free water pool. Figuratively speaking, longitudinal magnetization "flows" toward the pool with the larger T1 relaxation "sink." At very high magnetic fields T2 is also shortened by the chemical shift exchange (14). Although there is no transfer of transverse magnetization (39), it appears that T2 cross-relaxation by the adjacent macromolecular protons may be significant (14, 21).

At MR imaging field strengths immobility favors T2 shortening of the free water and even more so of the protons of the immobile structures. The very short T2 of the immobile protons (<1 msec) makes them invisible with standard MR imaging techniques. However the very short T2 of the immobile protons permits their preferential saturation with off-resonance irradiation. This saturation is passed from the immobile protons to the free water protons by longitudinal magnetization transfer, resulting in a decrease in the free water signal (15, 16, 20, 21). Saturation transfer allows detection and measurement of magnetization transfer. Clotting by itself had no effect on the AMTRs or relaxation rates of packed diamagnetic blood samples. This indicates that the fibrin mesh does not have a significant long-term hydration layer and or that fibrin polymerization does not affect the slow-motion components of the fibrin monomers or of the hemoglobin molecules (27).

The increase in the AMTR and T2 relaxation rate with marked increase in osmolality and pH is caused by red cell dehydration, which increases the intracellular hemoglobin concentration of the packed samples (41–45). Although pH also affects the relaxation rates of free hemoglobin solutions, the effect of pH on cell volume is dominant (46–48). Actually, the effects of pH on red cell volume are mediated by changes in osmolality (48, 49). These dehydrating effects do not appear to be significant in the physiologic range of osmolality and pH (42, 48, 49, 50). The obligatory increase in AMTR and 1/T2 of the hypothesized red cell dehydration due to aging of the red cell membranes (23) was not observed.

Clot retraction does increase the protein concentration, as does sedimentation. Nonetheless, compact packed diamagnetic clots which have a CT density more than twice that of brain had AMTRs one-third that of gray matter and one-fifth that of white matter. On the other hand, their T1 and T2 relaxation rates were similar to gray matter. It is unlikely that the differences in AMTR are caused by differences in extent of hydrogen bonding. Therefore, these findings indicate that the high hemoglobin concentration rather than the immobilization of hemoglobin is responsible for the relaxation rates of compact diamagnetic hematomas. In other words, a compact hematoma has the MR properties of a concentrated protein solution and not of tissue.

That blood does not behave like tissue on MR is not by chance. It has a physiologic purpose; maximization of oxygen transport. There is a close correlation between the rheologic and MR properties of protein molecules. The high concentration of intracellular hemoglobin is actually at a physiologic limit. Despite this high concentration, the lack of organelles and other macromolecular features of nucleated cells ensures blood's low viscosity and AMTR (17). Above the normal intracellular hemoglobin concentration of 34 g/100

TABLE 3: Intensity ratios of the blood and plasma samples to the gray matter (GM) and white matter (WM) of the brain in the three images of Figure 1

TR/TE	Hb				MHb			HbCO			Plasma		
	1 UI	2 UL	3 CI	4 CL	5 UI	6 UL	7 CI	8 CL	9 UI	10 UL	11 CI	12 CL	13 U	14 C	15 RC
500/20															
WM	1.01 ± 0.07	1.53 ± 0.06	1.02 ± 0.04	1.84 ± 0.06	1.84 ± 0.06	2.42 ± 0.05	1.82 ± 0.05	1.84 ± 0.07	1.04 ± 0.09	1.38 ± 0.05	0.97 ± 0.05	1.46 ± 0.05	0.75 ± 0.04	0.75 ± 0.05	0.87 ± 0.05
GM	1.22 ± 0.08	1.85 ± 0.06	1.24 ± 0.04	1.76 ± 0.05	2.23 ± 0.06	2.93 ± 0.06	2.20 ± 0.06	2.23 ± 0.08	1.26 ± 0.10	1.67 ± 0.06	1.18 ± 0.05	1.77 ± 0.06	0.91 ± 0.04	0.90 ± 0.04	1.05 ± 0.05
3000/20															
WM	1.25 ± 0.08	1.39 ± 0.06	1.21 ± 0.03	1.49 ± 0.04	1.44 ± 0.04	1.41 ± 0.04	1.27 ± 0.03	1.14 ± 0.08	1.22 ± 0.09	1.37 ± 0.04	1.18 ± 0.06	1.40 ± 0.04	1.24 ± 0.03	1.31 ± 0.03	1.51 ± 0.10
GM	1.14 ± 0.07	1.27 ± 0.05	1.10 ± 0.03	1.36 ± 0.04	1.31 ± 0.04	1.29 ± 0.03	1.16 ± 0.03	1.04 ± 0.04	1.11 ± 0.08	1.25 ± 0.03	1.08 ± 0.06	1.28 ± 0.04	1.13 ± 0.03	1.20 ± 0.04	1.38 ± 0.09
3000/90															
WM	1.50 ± 0.15	2.02 ± 0.09	1.20 ± 0.09	2.20 ± 0.11	1.67 ± 0.07	1.58 ± 0.06	0.91 ± 0.06	1.44 ± 0.11	1.64 ± 0.14	1.93 ± 0.07	1.72 ± 0.19	1.95 ± 0.07	2.94 ± 0.07	3.02 ± 0.08	2.82 ± 0.04
GM	1.08 ± 0.12	1.45 ± 0.08	0.86 ± 0.08	1.58 ± 0.09	1.20 ± 0.06	1.14 ± 0.06	0.66 ± 0.06	1.03 ± 0.09	1.18 ± 0.11	1.38 ± 0.06	1.23 ± 0.14	1.40 ± 0.07	2.11 ± 0.07	2.17 ± 0.07	2.02 ± 0.05

Note.—Hb = deoxyhemoglobin; MHb = methemoglobin; HbCO = carbonmonoxyhemoglobin; U = unclotted; C = clotted; RC = retracted plasma clot; I = intact red cells; L = lysed red cells.

ml viscosity rises very steeply, interfering with circulation (35, 51, 52). Increased viscosity is paralleled by decreased mobility (42, 52, 53) of the hemoglobin molecule, which is manifest by increased AMTR and T2 relaxation rate (Table 2). For comparison, Table 5 shows the magnetization transfer and relaxation rate data for three concentrated solutions of BSA, whose molecular weight almost equals that of hemoglobin. Note the similarly rapid increase in AMTR and T2 relaxation rate with increasing concentration (52, 54). In summary, as intracellular hemoglobin concentration rises above its normal levels, blood becomes more tissue like and much more viscous. The concentration and viscosity limit of hemoglobin is exceeded clinically in spherocytosis. In sickle cell disease hemoglobin polymerization greatly increases the T2 relaxation rate (50, 55), and presumably the AMTR, because of decreased mobility of sickle hemoglobin polymer (46). Hematomas of patients with spherocytosis and even more so with sickle cell disease should have significantly higher AMTRs. However, their T2 relaxation rates also will depend on magnetic susceptibility heterogeneity.

The relative insensitivity of the T1 relaxation rate at high magnetic fields to slow motion is demonstrated by the slower rise in 1/T1 with increasing hemoglobin and BSA concentrations (Tables 2 and 5). However, low magnetic field strengths increase the intrinsic T1 relaxation rates of both the free water protons and of the immobile protons. The linkage of the two proton pools by magnetization transfer serves to enhance further the free water proton pool relaxation rate (17, 22, 24, 46, 57). This increased 1/T1 may be responsible for the hyperintensity that has been reported on T1-weighted images of compact acute hematomas at ultra-flow–field MR (6).

The increase in T1 relaxation rate with red cell lysis has been observed before (2, 57), especially when the lysis by freeze thawing. Why others using different methods of cell lysis have not observed this effect (25, 33, 46, 58, 59) is unclear. The fact that AMTR and T2 relaxation rate are relatively unaffected suggests an increase in the rapid motional components of the free water molecules, near the proton resonant frequency. Whatever the mechanism of this phenomenon, it should not be relevant clinically, because most red cell lysis occurs in the subacute phase of hematomas when the T1 relaxation is dominated by methemoglobin.

TABLE 4: The change in 1/T1 of the blood samples with time

1/T1 (sec^{-1})	Hb				MHb				HbCO			
	1 UI	2 UL	3 CI	4 CL	5 UI	6 UL	7 CI	8 CL	9 UI	10 UL	11 CI	12 CL
Day 1	1.06 ± 0.01	1.49 ± 0.02	0.88 ± 0.04	1.03 ± 0.06	4.22 ± 0.45	4.90 ± 0.78	3.79 ± 0.23	4.03 ± 0.20	0.91 ± 0.02	1.21 ± 0.03	1.04 ± 0.12	1.15 ± 0.02
Week 2	1.21 ± 0.02	2.74 ± 0.10	1.05 ± 0.04	2.03 ± 0.07	2.41 ± 0.08	4.76 ± 0.89	2.28 ± 0.05	3.89 ± 0.11	1.20 ± 0.05	1.61 ± 0.04	1.16 ± 0.02	2.19 ± 0.04
Week 4	1.23 ± 0.05	2.44 ± 0.06	0.99 ± 0.01	2.80 ± 0.17	1.89 ± 0.09	5.81 ± 1.09	1.63 ± 0.03	3.46 ± 0.07	1.01 ± 0.03	1.27 ± 0.01	1.10 ± 0.03	2.57 ± 0.07
Week 8	1.18 ± 0.06	1.96 ± 0.06	1.42 ± 0.04	3.58 ± 0.76	1.36 ± 0.13	5.04 ± 0.08	1.37 ± 0.04	5.04 ± 0.35	1.02 ± 0.28	0.99 ± 0.05	1.15 ± 0.04	4.00 ± 0.42

Note.—Hb = deoxyhemoglobin; MHb = methemoglobin; HbCO = carbonmonoxyhemoglobin; U = unclotted; C = clotted; RC = retracted plasma clot; I = intact red cells; L = lysed red cells.

Retracted clot appears to pack less efficiently and regularly than does uncoagulated blood. If this occurs in vivo, clots may be associated with greater T2 shortening, because of susceptibility heterogeneity, rather than compact unclotted hematomas. Conversely, some compact unclotted partially deoxygenated hematomas may have a low enough susceptibility heterogeneity and high enough hemoglobin concentration to account for those hyperacute hematomas that are isointense to white matter on T1-weighted images and hyperintense to white matter on T2-weighted images.

Our in vitro aging of the blood samples was mostly at an unphysiologic 4°C. Nonetheless, it demonstrated interesting findings. There was an increase in T1 relaxation rates of the deoxyhemoglobin and carbonmonoxyhemoglobin samples, especially in the lysed clotted samples. A reverse effect with decrease in the T1 relaxation rate was observed in the methemoglobin samples with intact red cells (Table 4). These findings appear to be due to the oxidation of the deoxyhemoglobin and carbonmonoxyhemoglobin samples to methemoglobin and to a reduction of the methemoglobin in the methemoglobin samples (33). This suggests that the presence of unsedimented membrane fragments (lysed clot) accelerates methemoglobin formation overcoming the red cell's methemoglobin reductase activity. Although a specific mechanism for this is speculative, perhaps oxidation by free radicals associated with the unsedimented membrane fragments

TABLE 5: Magnetization transfer and relaxation rate data for solutions of BSA

	BSA Protein Weight Fractions		
	0.20	0.33	0.50
AMTR (sec^{-1})	0.11 ± 0.01	0.90 ± 0.20	6.27 ± 1.67
1/T2 (sec^{-1})	9.0 ± 0.1	21.7 ± 0.1	81.3 ± 0.8
1/T1 (sec^{-1})	0.71 ± 0.10	1.58 ± 0.07	4.26 ± 0.48
$1/AT1_{sat}$ (sec^{-1})	0.86 ± 0.08	2.47 ± 0.28	8.72 ± 0.45
AMTC (%)	12.1 ± 0.7	36.2 ± 4.0	60.5 ± 0.4

TABLE 6: Magnetization transfer and relaxation rate data for the gray matter (GM) and white matter (WM) of the volunteer's brain

	Brain	
	GM	WM
AMTR (sec^{-1})	0.9 ± 0.1	1.5 ± 0.2
1/T2 (sec^{-1})	17 ± 1	17 ± 2
1/T1 (sec^{-1})	1.0 ± 0.1	1.3 ± 0.2
$1/AT1_{sat}$ (sec^{-1})	1.9 ± 0.1	3.0 ± 0.3
AMTC (%)	46.8 ± 0.8	48.8 ± 2.5

plays a role in the process. The slower formation of methemoglobin in the intact carbonmonoxyhemoglobin samples than in the deoxyhemoglobin samples may be related to the need of methemoglobin reductase for oxygen (33), which was excluded from the deoxyhemoglobin samples. Clinical observations indicate that intracellular methemoglobin is a short lived phase in hematoma evolution suggesting that most methemoglobin production in hematomas may also be catalyzed by cell lysis.

Both the 1/T2 and AMTR are sensitive to the slowness of motion. However, comparison of the AMTRs and 1/T2s of the compact hematomas with those of gray and white matter, the BSA solutions, and the hypersomolar blood samples shows that the AMTR is more sensitive to macromolecular immobility or the amount of structure present in the sample. Thus, at high-field MR, it appears that the AMTR is most sensitive to immobility or extremely low frequency motion, and the 1/T1 is most sensitive to higher frequency motion, near the proton-resonant frequency of the magnetic field. Also, the AMTR is relatively independent of paramagnetic and susceptibility effects. Therefore, the AMTR is an important parameter, in addition to the T1 and T2 relaxation rates, in the analysis of the underlying mechanisms of tissue relaxation.

The AMTC is a measure of the decrease in the free water signal upon partially selective saturation of the immobile macromolecular protons by off-resonance irradiation. It increases with the rate of magnetization transfer and decreases when the 1/T1 of the free water protons increases, as with paramagnetic methemoglobin and Gd-DTPA. It is a less accurate indicator of the magnetization transfer than the AMTR, although its measurement is somewhat simpler. The technical limitations to measuring the magnetization transfer clinically are mentioned in "Materials and Methods."

Conclusion

Excluding the dominant paramagnetic effects, the next most important factor contributing to the appearance of hematomas on MR is the hemoglobin concentration, which does not appear to surpass that of packed red cells (34 g/100 ml). At this concentration diamagnetic hematomas have an intensity below or near that of white matter on T1-weighted images and above or near that of gray matter on T2-weighted images. Any lower protein concentration will lead to a lower intensity on T1-weighted images and higher intensity on T2-weighted images. The AMTR measurements show that compact contracted clots have the MR behavior of mobile protein solutions, without tissue-like macromolecular structure.

Acknowledgments

We acknowledge the useful discussions regarding magnetization transfer with Robert Lenkinski, PhD, and thank Karen Raemer, RT, and Norman Butler, RT, for help with performing the studies.

References

1. Gomori JM, Grossman RI, Goldberg HI, Zimmerman RA, Bilaniuk LT. Intracranial hematomas: imaging by high-field MR. *Radiology* 1985;157:87–93
2. Gomori JM, Grossman RI, Yu-Ip C, Asakura T. NMR relaxation times of blood: dependence on field strength, oxidation state, and cell integrity. *J Comput Assist Tomogr* 1987;11:684–690
3. Edelman RR, Johnson K, Buxton R, et al. MR hemorrhage: a new approach. *AJNR: Am J Neuroradiol* 1986;7:751–756
4. Atlas SW, Mark AS, Grossman RI, Gomori JM. Intracranial hemorrhage: gradient echo MR imaging at 1.5T—comparison with spin-echo imaging and clinical applications. *Radiology* 1988;168:803–807
5. Seidenwurm D, Meng T-K, Kowalski H, Weinreb JC, Kricheff II. Intracranial hemorrhagic lesions: evaluation with spin-echo and gradient-refocused MR imaging at 0.5 and 1.5 T. *Radiology* 1989;172:189–194
6. Sipponen JT, Sepponen RE, Tanttu JI, Sivula A. Intracranial hematomas studied by MR imaging at 0.17 and 0.02 T. *J Comput Assist Tomogr* 1985;9:698–704
7. Hallenga K, Koenig SH. Protein rotational relaxation as studied by solvent ^{1}H and ^{2}H magnetic relaxation. *Biochemistry* 1976;15:4255–4264
8. Fung BM. Proton and deuteron relaxation of muscle water over wide ranges of resonance frequencies. *Biophys J* 1977;18:235–239
9. Koenig SH, Bryant RG, Hallenga K, Jacob GS. Magnetic cross-relaxation among protons in protein solutions. *Biochemistry* 1978;17:4348–4358
10. Edzes HT, Samulski ET. The measurement of cross-relaxation effects in the proton NMR spin-lattice relaxation of water in biological systems: hydrated collagen and muscle. *J Magn Reson* 1978;31:207–229
11. Escanye JM, Canet D, Robert J. Nuclear magnetic relaxation studies of water in frozen biological tissues. Cross-relaxation effects between protein and bound water protons. *J Magn Reson* 1984;58:118–131
12. Sobol WT, Cameron IG, Inch WR, Pintar MM. Modeling of proton spin relaxation in muscle tissue using nuclear magnetic resonance spin groupings and exchange analysis. *Biophys J* 1986;50:181–191
13. Koenig SH, Brown RD. The raw and the cooked, or the importance of the motion of water for MRI revisited. *Invest Radiol* 1988;23:495–497
14. Zhong J, Gore JC, Armitage IM. Relative contributions of chemical exchange and other relaxation mechanisms in protein solutions and tissues. *Magn Reson Med* 1989;11:295–308
15. Wolff SD, Balaban RS. Magnetization transfer contrast (MTC) and tissue water proton relaxation in vivo. *Magn Reson Med* 1989;10:135–144

16. Ceckler TL, Wolff SD, Yip V, Simon SA, Balaban RS. Dynamic and chemical factors affecting water proton relaxation by macromolecules. *J Magn Reson* 1992;98:637–645
17. Koenig SH, Brown RD. Field-cycling relaxometry of protein solutions and tissue: implications for MRI. *Prog NMR Spectroscopy* 1990;22:487–567
18. Koenig SH, Brown RD, Ugolini R. A unified view of relaxation in protein solutions and tissue, including hydration and magnetization transfer. *Magn Reson Med* 1993;29:77–83
19. Zhong J, Gore JC, Armitage IM. Quantitative studies of hydrodynamic effects and cross-relaxation in protein solutions and tissues with proton and deuteron longitudinal relaxation times. *Magn Reson Med* 1990;13:192–203
20. Eng J, Ceckler TL, Balaban RS. Quantitative ^{1}H magnetization transfer as a probe of cross relaxation aqueous lipid bilayer suspensions. *Magn Reson Med* 1991;17:304–314
21. Ceckler TL, Balaban RS. Tritium-proton magnetization transfer as a probe of cross relaxation in aqueous lipid bilayer suspensions. *J Magn Reson* 1991;93:572–588
22. Gallier J, Rivet P, de Certaines J. ^{1}H- and ^{2}H-NMR study of bovine serum albumin solutions. *Biochim Biophys Acta* 1987;915:1–18
23. Hayman LA, Taber KH, Ford JJ, Bryan RN. Mechanisms of MR signal alteration by acute intracerebral blood: old concepts and new theories. *AJNR: Am J Neuroradiol* 1991;12:899–907
24. Koenig SH, Brown RD, Adams D, Emerson D, Harrison CG. Magnetic field dependence of 1/T1 of protons in tissue. *Invest Radiol* 1984;19:76–81
25. Nummi P, Alanen A, Nanto V, Kormano M. Effect of hemolysis and clotting on proton relaxation times of blood. *Acta Radiol Diagn* 1986;27:225–230
26. Sostman D, Pope CF, Smith GJW, Carbo P, Gore JC. Proton relaxation in experimental clots varies with method of preparation. *Invest Radiol* 1987;22:509–512
27. Blinc A, Lahajnar G, Blinc R, Zidansek A, Sepe A. Proton NMR study of the state of water in fibrin gels, plasma, and blood clots. *Magn Reson Med* 1990;14:105–122
28. Bryant RG, Marill K, Blackmore C, Francis C. Magnetic relaxation in blood and blood clots. *Magn Reson Med* 1990;13:133–144
29. Clark RA, Watanabe AT, Bradley WG, Roberts JD. Acute hematomas: effects of deoxygenation, hematocrit and fibrin-clot formation and retraction on T2 shortening. *Radiology* 1990;175:201–206
30. Janick PA, Hackney DB, Grossman RI, Asakura T. MR imaging of various oxidation states of intracellular and extracellular hemoglobin. *AJNR: Am J Neuroradiol* 1991;12:891–897
31. Daszkiewicz OK, Hennel JW, Lubas B. Proton magnetic relaxation and protein hydration. *Nature* 1963;200:1006–1007
32. Thulborn KR, Waterton JC, Matthews PM, Radda GK. Oxygenation dependence of transverse relaxation time of water protons in whole blood at high field. *Biochim Biophys Acta* 1982;714:265–270
33. Bass J, Sostman HD, Boyko O, Koepke JA. Effects of cell membrane disruption on the relaxation rates of blood and clot with various methemoglobin concentrations. *Invest Radiol* 1990;25:1232–1237
34. Fabry TL, Reich HA. The role of water in deoxygenated hemoglobin solutions. *Biochem Biophys Res Commun* 1966;22:700–703
35. Chien S, Usami S, Bertles JF. Abnormal rheology of oxygenated blood in sickle cell anemia. *J Clin Invest* 1970;49:623–634
36. Caines GH, Goldstein JH. NMR investigation of hydroxyethyl starch-induced aggregation of human erythrocytes. *Magn Reson Med* 1987;5:67–72
37. Hardeman MR, Goedhart P, Koen IY. The effect of low-osmolar ionic and nonionic contrast media on human blood viscosity, erythrocyte morphology and aggregation behavior. *Invest Radiol* 1991;26:810–819
38. Outwater E, Schnall MD, Braitman LE, Dinsmore BJ, Kressel HY. Magnetization transfer of hepatic lesions: evaluation of a novel contrast technique in the abdomen. *Radiology* 1992;182:535–540
39. Solomon I. Relaxation processes in a system of two spins. *Phys Rev* 1955;99:559–565
40. Forsen S, Hoffman RA. Study of moderately rapid chemical exchange reaction by means of nuclear magnetic double resonance. *J Chem Phys* 1963;39:2892–2901
40.a Listinsky. Models of solidlike protein protons in magnetization transfer imaging (abstr). *Radiology* 1992;185P:303
41. Fabry ME, Eisenstadt M. Water exchange across red cell membranes: II. Measurement by nuclear magnetic resonance T1, T2, and T12 hybrid relaxation. The effects of osmolarity, cell volume, and medium. *J Membrane Biol* 1978;42:375–398
42. Eisenstadt M, Fabry ME. NMR relaxation of hemoglobin-water proton spin system in red blood cells. *J Magn Reson* 1978;29:591–597
43. Zipp A, James TL, Kuntz ID, Shohet SB. Water proton magnetic resonance studies of normal and sickle erythrocytes. Temperature and volume dependence. *Biochim Biophys Acta* 1976;428:291–303
44. Bull BS, Breton-Gorious J, Beutler E. Morphology of the erythron. In: Williams WJ, Beutler E, Erslev AJ, Lichtman MA, eds. *Hematology.* New York: McGraw-Hill, 1990:297–316
45. Bull BS, Brailsford D. Red blood cell shape. In: Agre P, Parker JC, eds. *Red blood cell membranes. Structure. Function. Clinical implications.* New York: Marcel Dekker, 1990:401–421
46. Lindstrom TR, Koenig SH. Magnetic-field dependent water proton spin-lattice relaxation rates of hemoglobin solutions and whole blood. *J Magn Reson* 1974;15:344–353
47. Brooks RA, Battolcletti JH, Sances A Jr, Larson SJ, Bowman RL, Kudravieu V. Nuclear magnetic relaxation in blood. *IEEE Trans on Biomed Engr* 1974;BME22:12–18
48. Hansen AT. Osmotic pressure effect of the red blood cells—possible physiologic significance. *Nature* 1961;190:504–508
49. Rand PW, Austin WH, Lacombe E, Barker N. pH and blood viscosity. *J Appl Physiol* 1968;25:550–559
50. Zipp A, Kuntz ID, Rehfeld SJ, Shohet SB. Proton magnetic resonance studies of intracellular water in sickle cells. *FEBS Lett* 1974;43:9–12
51. Erslev AJ, Atwater J. Effect of mean corpuscular hemoglobin concentration on viscosity. *J Lab Clin Med* 1963;62:401–406
52. Kamman RI, Go KG, Brouwer W, Berendsen HJC. Nuclear magnetic resonance relaxation in experimental brain edema: effects of water concentration, protein concentration, and temperature. *Magn Reson Med* 1988;6:265–274
53. Lindstrom TR, Koenig SH, Boussios T, Bertles JF. Intermolecular interactions of oxygenated sickle hemoglobin molecules in cells and cell-free solutions. *Biophys J* 1976;16:679–689
54. Grosch L, Noack F. NMR relaxation investigation of water mobility in aqueous bovine serum albumin solutions. *Biochim Biophys Acta* 1976;453:218–232
55. Cottam GL, Valentine KM, Yamaoka K, Waterman MR. The gelation of deoxyhemoglobin S in erythrocytes as detected by transverse water proton relaxation measurements. *Arch Biochem Biphys* 1974;162:487–492
56. Thompson BC, Waterman MR, Cottam GL. Evaluation of the water environments in deoxygenated sickle cells by longitudinal and transverse water proton relaxation rates. *Arch Biochem Biophys* 1975;166:93–200
57. Singer JR, Crooks LE. Some magnetic studies of normal and leukemic blood. *J Clin Engr* 1978;3:237–243
58. Finnie M, Fullerton GD, Cameron IL. Molecular masking and unmasking of the paramagnetic effect of iron on the proton spin-lattice (T1) relaxation time in blood and blood clots. *Magn Reson Imag* 1986;4:305–310
59. Cohen MD, McGuire W, Cory DA, Smith JA. MR appearance of blood and blood products: an in vitro study. *AJR: Am J Roentgenol* 1986;146:1293–1297